

A Study on Nucleation, Growth and Shrinkage of Oxidation Induced Stacking Faults(OSF)

-Part 1 : Nucleation and Thermal Behavior of Oxidation Induced Stacking Faults(OSF)

(산화 적층 결함의 생성, 성장 및 소멸에 관한 연구
- 제 1부 : 산화 적층 결함의 생성과 열적 거동)

金 龍 泰*, 金 春 權*, 閔 碩 基*

(Yong Tae Kim, Chun Keun Kim and Suk Ki Min)

要 約

n형 (100) 실리콘 웨이퍼의 산소 분위기 속에서 열처리에 따른 산화 적층 결함의 생성과 성장을 조사하였다. 산화 적층 결함의 성장은 실리콘 웨이퍼의 산소농도, 열처리 시간 및 온도에 의존하며 따라서, 성장기구에 대한 간단한 해석으로부터 결함의 성장에 필요한 활성화 에너지를 구할 수 있었다. 또한 본 연구에서는 산화 적층 결함의 결정학적 구조 및 Nomarski 간섭 현미경 관찰의 비교 분석을 통하여 적층 결함의 구조적 특징을 살펴보았다.

Abstract

The effect of heat treatment in oxygen ambient on the nucleation and growth of oxidation induced stacking faults (OSF) in n-type (100) silicon wafer has been investigated. The growth of OSF is determined as a function of oxygen concentration in silicon wafer, heat treatment time and temperature, and the activation energy for the growth of OSF can be obtained from the growth kinetics. The activation energies are respectively 2.66 eV for dry oxidation and 2.37 eV for wet oxidation. In this paper, we have also studied the structural feature of OSF with the comparison of optical microscopic morphology and crystalline structure.

*正會員, 韓國科學技術院 半導體 材料研究室
(Semicond. Materials Lab., KAIST)
接受日字: 1988年 2月 10日

I. Introduction

Great advances in silicon industries are to be possible due to the development of VLSI tech-

nology, which demands precise control of physical, chemical and electrical properties of silicon material. This is because the state of crystalline perfection affects device performance. Now, the silicon wafer manufacturing technology has been improved over past decades, conventional defects, such as dislocations, twins and other large defects, have become greatly reduced. However, microdefects, which are inevitably induced during crystal growth and process induced defects, which are generated during sequential device fabrication processes and potential defect nuclei, still remain as the focus of intensive research [1-11]. Particularly, since OSF is known to be nucleated from the grown-in microdefects introduced during CZ growth and it grows due to the processing such as oxidation and diffusion, many authors have reported the theoretical analysis and experimental results of OSF for several years [2], [6], [8], [12-19].

In this paper, we have discussed not only the growth kinetics of OSF but also the morphological

features of the defect.

II. Experimental

We have grown (100) orientation, phosphorus doped silicon ingots by CZ method. The range of resistivity of this ingots is 2 to 4 ohm-cm. Wafers of 500 μm thickness, were cut out from the three different portions of each ingot such as seed, body and tail. These wafers were appled and polished with the chemo-mechanical method. After that, the final thickness of all wafers was $390 \mu\text{m} \pm 5 \mu\text{m}$.

In order to determine the influence of oxygen concentration on the OSF, all samples obtained from each portion of the same ingot were checked by FTIR measurement. The nucleation and growth of OSF were studied according to the heat treatment procedures, as seen in Table 1. Morphology and structure of OSF were investigated with Nomarski interference microscope and SEM.

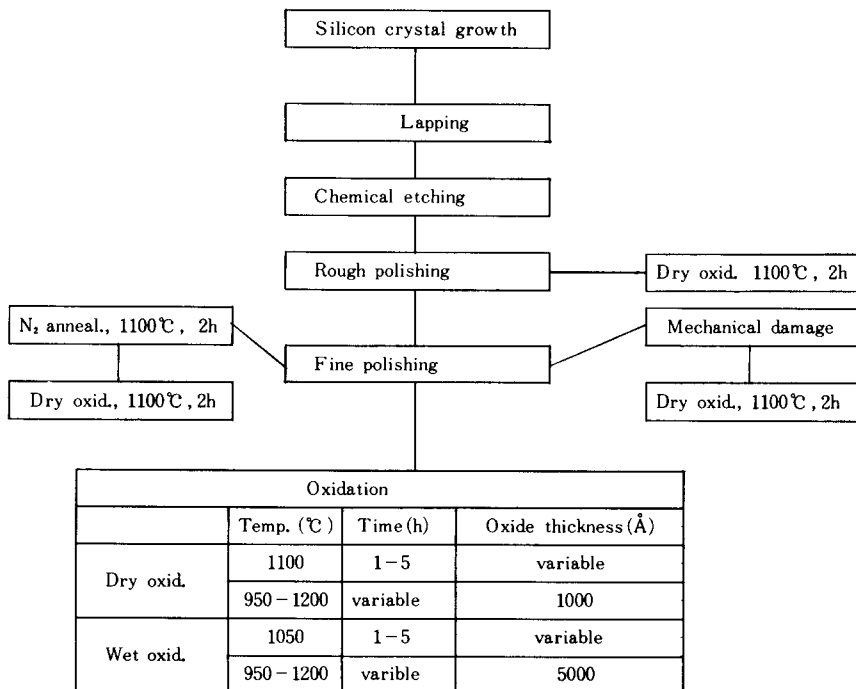


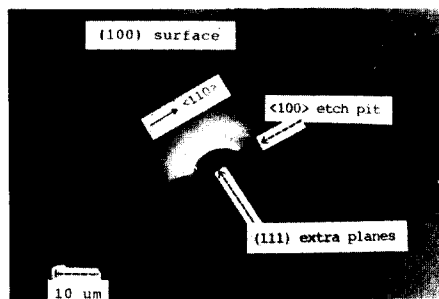
Fig.1. Experimental producedures.

III. Results and Discussion

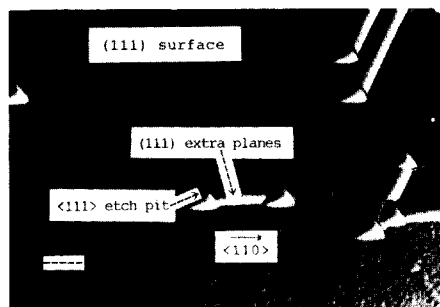
1. Morphology and structure of OSF

It is well known that the observation of OSF is done with TEM, which needs a extremely hard work for sample preparation [9].[15]. However, in this paper, we observed morphology and structure of OSF only with Nomarski interference microscope, the careful chemical etching method, and X-ray measurement. Chemical etchant was the conventional Wright solution [20-21], but we added 5 gms of silicon piece into 100cc solution and used it after one day in order to reduce the activity of the solution[22].

Fig.2 shows that OSF is in the (111) planes and these (111) planes intersect the surface of (100) Si wafer along the $[110]$ direction. In this picture, we can find clearly two etch pit dislocations occurred at the edge of OSF. This fact indicates that, as Friedel [23-24] have suggested, a jog occurs due to two dislocation intersection



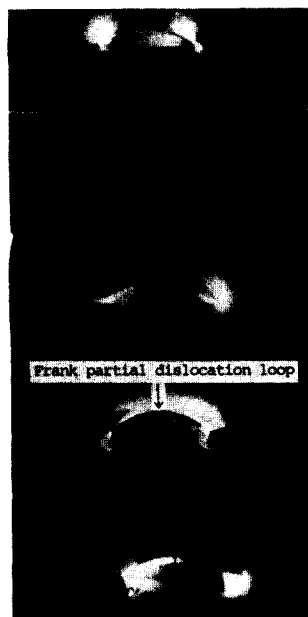
(a)



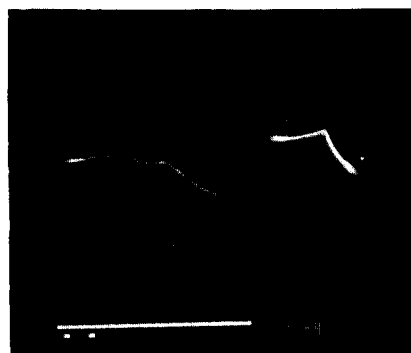
(b)

Fig.2. (a) Micrograph of OSF on (100) silicon surface.
(b) Micrograph of OSF on (111) silicon surface.

in the fcc lattice and it splits into partial dislocations such as a Frank and a Shockley partial. As these extended jogs, the Shockley partial, move away from the Frank, the immobility of the Frank forces the motion of dislocation to be non-conservative. Therefore, the Frank partial dislocation trails behind the moving dislocation line. We can understand the above fact after investigating Fig. 3, which shows that fault is



(a)



(b)

Fig.3. (a) Sequential micrographs of OSF representing the Frank partial dislocation loop.
(b) Scanning electron micrograph of OSF representing 3-D structure.

bounded by the Frank partial edge dislocation of $1/3 \langle 111 \rangle$ type. This is revealed by step preferential etching, X-ray Laue diffraction measurement, and Nomarski interference microscope. The nail-tip-like shape shows the (100) plane and the edge of the round shape is $1/3 \langle 111 \rangle$ type dislocation loop. After step etching, the dislocation loop apparently appeared.

2. Nucleation of OSF

We have tried to establish a correlation between the nucleation of OSF and the interstitial oxygen concentration. Radial and axial concentrations of oxygen are measured by FTIR spectrometer (QS 100 digilab.). the axial distribution of oxygen concentration and OSF density from the three different portions of ingot are summarized in Fig.4. It is found that while the distribution of oxygen concentration gets generally lower toward the body part due to the oxygen segregation effect[25], oxygen concentration of the tail part is higher than that of the body part because oxygen is believed to be continuously dissolved from the quartz crucible during the crystal growth[25]. As the result of the oxygen concentration distribution, the distribution of OSF density also shows the same tendency. Like the interstitial oxygen atoms, microdefects and mechanical damages are also known to act as the nucleation sites for OSF. Especially, we paid a great attention to the role of microdefects in the formation of OSF in this study. In this experiment, particularly, it is to confirm that OSF is originated from microdefect. Several wafers selected from the tail part of a ingot are heat

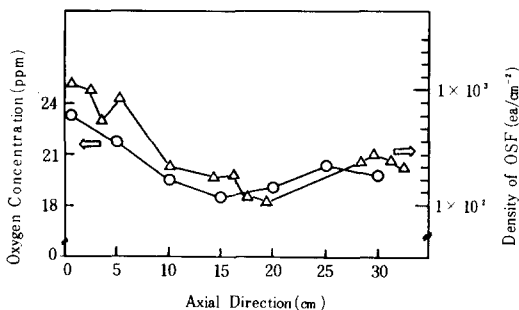


Fig.4. Relation of OSF density vs oxygen concentration.

treated to generate microdefects in the N_2 ambient at 1100 C for 2 hrs, which is followed by Wright etching. It is observed that microdefects are widely distributed across the whole wafer. Its density is very high and their sizes are in the submicron range. These samples are oxidized again in the O_2 ambient at 1100 C for 2 hrs. Micrographs in Fig.5 show that many OSFs are generated in the sample wafers.

Micrographs in Fig.6 show that OSFs are also generated either from the damages induced by the rough polishing process or along the scratch line that is intentionally drawn on the fine polished wafer surface. These kinds of OSF can be easily distinguished in the microdefects.

3. Growth of OSF

The growth of OSF occurs during the thermal oxidation of OSF. It is well known that silicon self-interstitials are generated the Si-SiO₂ interface as the result of incomplete half cell reaction involving silicon and oxygen during oxidation process[11-14],[16-17],[19]. These silicon interstitials produce an extra plane of atoms between the closely packed (111) planes[12-13],[15],[17],[19]. There are also many other models available to explain the growth mechanism of OSF[12-13],[17],[19],[24]. In this paper, however, we propose that the growth mechanism of OSF can be explained as the function of such parameters as concentration of interstitials, activation energy of the growth, oxygen partial pressure, oxidation time, and behavior of partial dislocation.

According to Leroy[17], if C_i , the concentration of silicon interstitials at a distance r from the partial dislocation established the fault line exceeds C_i^0 , the concentration of silicon interstitials, which is inside of Burgers vector, OSF grows due to the absorption of silicon interstitials during the motion of partial dislocation. Therefore, when $C_i > C_i^0$, the change in the length of OSF L per oxidation time t is:

$$dL/dt = k_1 \cdot \frac{C_i}{C_i^0} \cdot \exp(-H/kT) \quad (1)$$

Where k_1 depends on the reaction of partial dislocations and the oxygen partial pressure, H is the sum of the enthalpy of interstitial migration and that of interstitial formation C_i/C_i^0 will vary with oxidation time and oxygen partial pressure.

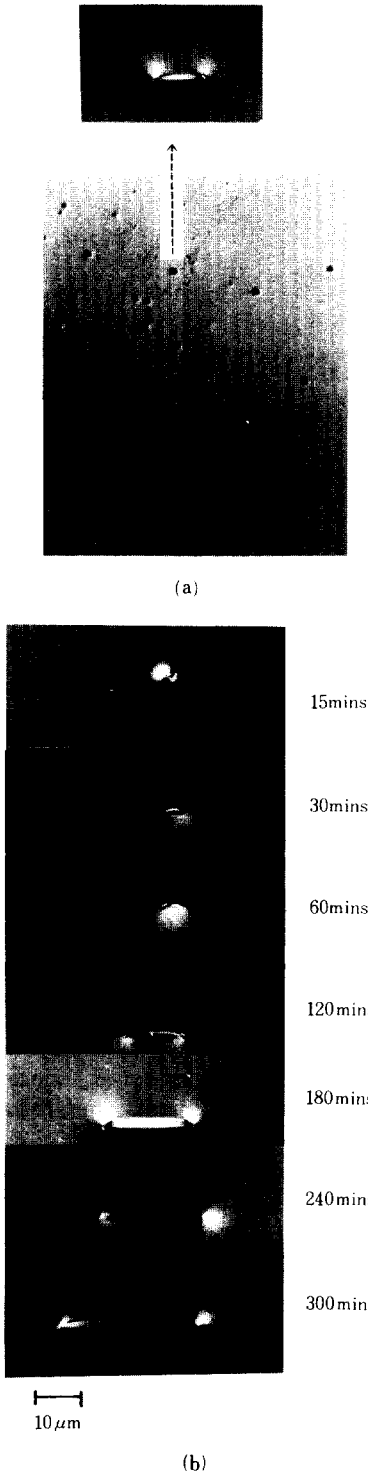


Fig.5. (a) Micrograph of OSF observed in the tail part of the ingot.
(b) Sequential micrographs of OSF representing the growth of OSF.

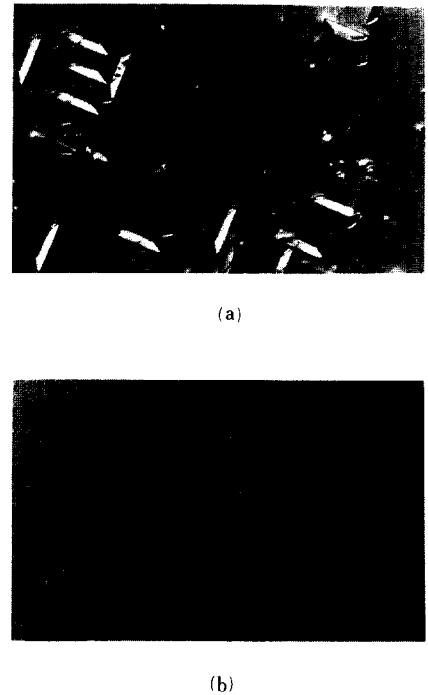


Fig.6. (a) Micrograph of OSF generated on the rough polished silicon surface.
(b) Micrograph of OSF generated on the scratch lines.

C_i/C_i^O can be written by the mass action law and Muraka's result[13] as following:

$$C_i/C_i^O = k_2 \cdot t^m \cdot p \cdot \exp(-H_s/kT) \quad (2)$$

Where k_2 , p and m depend on the oxygen partial pressure and the reaction of the Si-SiO₂ interface, H_s is the enthalpy for activating interstitial generation. After substituting Eq.(2) into Eq.(1), the integration of Eq.(1) gives Eq.(3)

$$L = \frac{k_1 \cdot k_2 \cdot p}{1 + m} \cdot t^{m+1} \cdot \exp(-(H + H_s)/kT) \quad (3)$$

Equation (3) can be simplified as Eq.(4)

$$L = k' \cdot t^n \cdot p \cdot \exp(-Q/k T) \quad (4)$$

Where k' is $k_1 \cdot k_2 / (1 + m)$, n equals to $(1+m)$ and Q is the activation energy for the growth of OSF. Empirically, we try to find the values of n and Q .

When oxygen partial pressure, oxidation temperature, and wafer orientation are fixed and only oxidation time is extended from 30 to 300 mins, n is calculated from Eq.(5)

$$L = t^n \quad (5)$$

Fig.7 shows that n is 0.81 in dry oxidation case and 0.67 in wet oxidation. Upon substituting these values into Eq.(4), the activation energy Q is also calculated from the Arrhenius relationship of growth and temperature, which is shown in Fig.8. The relationship can be obtained from Eq. (6), which is derived from Eq.(4), oxidation time, oxygen partial pressure and oxide thickness are fixed.

$$L/t^n = \exp(-Q/kT) \quad (6)$$

In dry oxidation case, the activation energy for the growth of OSF is 2.66 eV and for the wet oxidation case, the value is 2.37 eV. These values are similar to the results reported by other authors [12],[17],[19].

IV. Conclusion

We can ascertain that the morphology and structure of OSF are characterized by the careful Wright etching method. In the optical microscopic pictures, the dislocation intersection and the stacking faults established by Frank partial

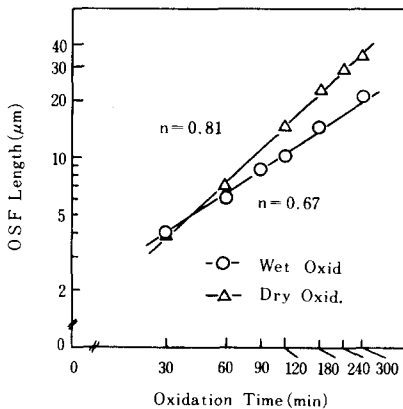


Fig.7. Relation of OSF length vs annealing time in both dry oxid. and wet oxidation.

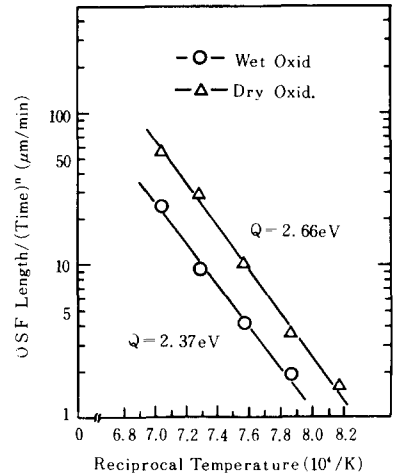


Fig.8. Arrhenius relation of OSF length per time vs reciprocal temperature.

dislocation are clearly revealed. There is some correlation between the interstitial oxygen concentration and the nucleation of OSF. Moreover, it is found that OSF is originated from the grown-in microdefects and the mechanical damages induced during wafering process. The activation energy for the growth of OSF is 2.66 eV in dry and 2.37 eV in wet oxidation case.

References

- [1] J. Matsui and T. Kawamura, "Spotty defects in oxidized floating zoned dislocation free silicon crystals," *Jpn. J. Appl. Phys.* vol. 11, no. 2, p. 197, Feb. 1972.
- [2] S. Prussin, "Role of sequential annealing, oxidation and diffusion upon defect generation in ion-implanted silicon surfaces," *Appl. Phys.* vol. 45, no. 4, p. 1635, Apr. 1974.
- [3] P.E. Freeland, et al, "Precipitation of oxygen in silicon," *Appl. Phys. Lett.* vol. 30, no. 1, p. 31, Jan. 1977.
- [4] L.C. Kimerling and J.R. Patel, "Defect states associated with dislocations in silicon," *Appl. Phys. Lett.*, vol. 34, no. 1, p. 73, Jan. 1979.
- [5] J. Chikawa and S. Yoshikawa, "Swirl defects in silicon single crystals," *Solid State Technol.*, p. 65, Jan. 1980.

- [6] S.P. Muraka, et al, "A study of stacking faults during CMOS processing: origin, elimination and contribution to leakage," *J. Electrochem. Soc.*, vol. 127, no. 3, p. 716, Mar. 1980.
- [7] S.M. Hu, "Precipitation of oxygen in silicon: some phenomena and a nucleation model," *J. Appl. Phys.* vol. 52, no. 6, p. 3975, June 1981.
- [8] F. Shimura and H. Tsuya, "Multi step repeated annealing for CZ-silicon wafers: oxygen and defect behavior," *J. Electrochem. Soc.*, vol. 129, no. 9, p. 2089, Sept. 1982.
- [9] C.A. Pimental and B.C. Brito Filho, "Point defect aggregates in boron doped dislocation free CZ silicon crystals," *J. Crystal Growth*, vol. 62, p. 129, 1983.
- [10] S.T. Chang, J.K. Wu, and S.A. Lyon "Amphoteric defects at the Si-SiO₂ interface," *Appl. Phys. Lett.*, vol. 48, no. 10, p. 662, Mar. 1986.
- [11] Y.T. Kim and S.K. Min, "Direct shrinkage observation of oxidation induced stacking faults in P-type CZ silicon," *Proc. 1986. Seoul Int. Symp. Phys. Semicond. & Appl.*, p. 153, 1986.
- [12] S.M. Hu, "A nomalous temperature effect of oxidation stacking faults in silicon," *Appl. Phys. Lett.* vol. 127, no. 4, p. 165, Aug. 1975.
- [13] S.P. Muraka, "Role of point defects in the growth of the oxidation induced stacking faults in silicon," *Phys. Rev. B*, vol. 16, no. 6, p. 2844, Sept. 1977.
- [14] G.A. Rozgonyi, "Silicon defect diagnostics and the wheel of misfortune," *Semicond. silicon*, 1977, p. 504, 1977.
- [15] O.L. Krivanek and D.M. Maher, "The core structure of extrinsic stacking faults in silicon," *Appl. Phys. Lett.* vol. 32, no. 8, p. 451, Apr. 1978.
- [16] H. Shimizu, et al, "Formation of stacking fault free region thermally oxidized silicon," *Jpn. J. Appl. Phys.* vol. 17, no. 5, p. 767, May 1978.
- [17] B. Leroy, "Kinetics of oxidation induced stacing faults," *J. Appl. Phys.* vol. 50, no. 12, p. 7996, Dec. 1979.
- [18] G. Charitat and A. Martinez, "Stress evolution and point defect generation during oxidation of silicon," *J. Appl. Phys.* vol. 55, no. 4, p. 909, Feb. 1984.
- [19] K. Nishi and D.A. Antoniadis, "Observation of silicon interstitial supersaturation during phosphorus diffusion from growth and shrinkage of oxidation induced stacking faults," *J. Appl. Phys.*, vol. 59, no. 4, p. 1117, Feb. 1986.
- [20] B. Shwatz and H. Robbins, "Chemical etching of silicon," *J. Electrochem. Soc.*, vol. 108, no. 4, p. 365, 1961.
- [21] M. Wright Jenkins, "A new preferential etch of defects in silicon crystal," *J. Electrochem Soc.*, vol. 124, no. 5, p. 757, May 1977.
- [22] Y.T. Kim and S.K. Min, "Crystal defects in silicon," *Proc. of the 6th Solid State Phys. Symp.*, p. 150, Aug. 1983.
- [23] K.V. Ravi, Imperfections and impurities in semiconductor silicon," John Wiley & Sons, 1981.
- [24] F.R.N. Nabaro, "Dislocations in solids," North-Holland Co., vol. 2, p. 81, 1979.
- [25] W. Lin and D.W. Hill, "Oxygen segregation in CZ silicon growth," *J. Appl. Phys.* vol. 54, no. 2, p. 1082, Feb. 1983. *

 著 者 紹 介


金 龍 泰(正會員)

1954年 3月 3日生. 1981年 2月
경북대학교 전자공학과 졸업(B.S)
1982年 2月 경북대학교 대학원 전
자공학과 석사학위 취득. 1982年
3月~12月 경북대학교 전자공학
과 강사. 1984年 3月~1987年 12
月 한국과학기술원 전기 및 전자공학과 박사과정. 현
재 한국과학기술원 반도체재료연구실 선임연구원
주관심분야는 PECVD, ECRCVD, RIE 기술, 3 차원
구조 VLSI 기술 등임.


閔 碩 基(正會員)

1938年 12月 14日生. 1964年 2月
고려대학교 물리학과 졸업 1966年
고려대학교 대학원 고체물리학 전
공 이학석사 학위 취득. 1968年 고
려대학교 물리학과 조교. 1969年~
1970年 고려대학교 물리학과 강사.
현재 한국과학기술원 반도체재료연구실 실장. 주
관심분야는 Si, GaAs 단결정성장기술 MOCVD, HEMT
관련기술 개발분야 등임.

●


金 春 權(正會員)

1957年 5月 20日生. 1988年 2月
한양대학교 대학원 전자공학과 석
사학위 취득. 현재 한국과학 기술
원 반도체재료연구실 연구원 주관
심분야는 PECVD, ECRCVD, RIE
기술 3 차원구조 VLSI 기술등임.